# Prediction of Propfan Noise by a Frequency-Domain Scheme

H. Gounet* and S. Lewy†
*Office National d'Etudes et de Recherches Aéronautiques, Châtillon, Cedex, France*

**The noise of single-rotating propfans is predicted from the solution of the Ffowcs Williams and Hawkings equation in the frequency domain. The computations under certification procedures are based on the concepts developed for conventional propellers because the flight speeds are low. Emphasis is put on noise computation on the fuselage outer wall at cruise speed. Since the helical tip velocities are then transonic, the previous codes must be completed to take into account the noncompactness of the acoustic sources and the blade twist. In addition, a method of estimation of near-field propeller sound levels is developed from the Euler three-dimensional equations. Finally, acoustic measurements on a 1-m model propfan in the S1-MA transonic wind tunnel of Modane-Avrieux are presented, and comparisons with theoretical results are given.**

## Nomenclature

$A$ = parameter related to the observer location
$B$ = number of propeller blades
$b$ = chord at span $r$
$c$ = sound velocity
$C_p$ = power coefficient, $W/(\rho N^3 D^5)$
$D$ = propeller diameter
$F(z)$ = span force distribution function
$f(z,x)$ = chord force distribution function
$h(x)$ = thickness along the chord
$H(x)$ = reduced thickness, $h(x)/b$
$J$ = advance ratio, $\pi M/M_{\text{rot}}$
$J_{mB}$ = first-kind Bessel function of order $mB$
$l$ = position along the chord
$M$ = advancing Mach number
$M_{\text{rot}}$ = rotational Mach number at blade tip, $\Omega R/c$
$M_{\text{rel}}$ = relative Mach number at blade tip, $(M^2_{\text{rot}} + M^2)^{1/2}$
$m$ = harmonic order
$N$ = propeller rotational frequency
$p$ = sound pressure
$p_l$ = loading noise
$p_t$ = thickness noise
$R$ = propeller radius, $D/2$
$r$ = position along the span
$S$ = modified observation distance, $[X^2 + \beta^2(Y^2 + Z^2)]^{1/2}$
$V$ = forward flight speed, $cM$
$W$ = power supplied to the propeller
$(X,Y,Z)$ = coordinates of observer location
$x$ = reduced chord, $l/b$
$z$ = reduced span (case of a plane blade), $r/R$
$\beta^2$ = $1 - M^2$
$\eta$ = propeller efficiency
$(\eta_1,\eta_2,\eta_3)$ = point source coordinates
$\rho$ = air density
$\varphi$ = parameter related to the observer location
$\psi_0$ = sweep angle of the blade (case of plane blades)
$\Omega$ = rotation speed of propeller

Received Jan. 8, 1987; revision received April 8, 1987. 

*Research Engineer, Physics Department.
†Chief of Aeroacoustics Subdivision, Physics Department.

## I. Introduction

PROPFANS offer the advantage of a higher propulsive efficiency than turbojet engines for flight Mach numbers of 0.7–0.8.[1,2] The resulting fuel savings are certain to be of interest for future short- and medium-range airplanes. It is for this reason that Aerospatiale, Ratier-Figeac, and ONERA have undertaken, under contracts with French government agencies, a research program concerning propfan aerodynamics, aeroelasticity, and acoustics. This paper refers to the acoustic design of this type of propellers; it is limited to the case of single-rotating propellers and marks a first step toward the study of counterrotating propellers and unducted fans, which appear at this time to be among the most probable aircraft solutions.

Propeller pure tone noise prediction codes have been developed at ONERA. Used in former research on propellers for light aircraft,[3,4] they have been applied to the calculation of propfan thickness and loading noise in the far field. Section II presents the sound level estimated by these programs under conditions of certification (far field, moderate flight speeds). Section III is devoted to the extension of the computations for cruise flight (noise on the fuselage, high advancing speeds). The improvements provided concern the thickness term, which, in this case, becomes predominant for single-rotating propellers. The noncompactness of the acoustic sources and the blade twist are included in this calculation.

This method, while entirely acceptable under the conditions of certification, is not completely satisfactory in the case of cruising for two reasons: on the one hand, the fuselage is located too close to the propeller for the far-field hypotheses to be totally valid; on the other hand, the quadrupole term, which becomes large at transonic helical tip speed,[5] mainly for unswept nontapered blades,[6] is not included in the calculations. For these reasons, predictions from aerodynamic calculations based on the Euler three-dimensional (3D) equations[7] are currently being developed: the mesh extends only to the vicinity of the blades, and the pressure fluctuations, determined only in near field, include all noise sources of aerodynamic origin. This idea, also utilized by Korkan and Von Lavante,[8] is described in Sec. IV.

Along with the theoretical studies, a 1-m-diam 12-bladed propeller model was tested in the ONERA S1-MA wind tunnel at Modane-Avrieux. The main objectives were to determine the performance and aerodynamic and aeroelastic characteristics of this model. Acoustic measurements were

also carried out, and some of the experimental results obtained from these tests are given in Sec. V.

## II. Far-Field Noise Computation Under Conditions of Certification

The details concerning the derivation of the expressions and the method used are outlined in Ref. 4. The propeller tone noise sources are broken down conventionally into monopoles (thickness noise), dipoles (loading noise), and quadrupoles. Only the expressions of thickness and loading noise are established. To this end, we expand the Lighthill wave equation in the integral form of Ffowcs Williams and Hawkings as modified by Goldstein[9] to take into account the motion of translation of the sources. The Fourier transform of the expressions leads to making the computations in the frequency domain, which directly gives the sound level of the tones. This method is quite close to that followed by Hanson,[10] although the latter is placed straight off in a fixed reference frame, whereas our calculations are worked out in a reference frame linked to the aircraft (origin at the center of the propeller). Likewise, Legendre[11] and Tam and Salikuddin[12] use the same basic equations to describe the noise generated by a propeller and a helicopter rotor, but with respect to a rotating reference frame (linked to the blades). The type of development followed in the present paper avoids singularities that appear at transonic speeds when calculating the solution of the wave equation in the time domain; denominators close to zero can then appear in the source terms. However, several means exist to solve these difficulties.[13-15]

For calculations under conditions of certification, the forward velocities and, thereby, the helical tip velocities are moderate. Some simplifying hypotheses can then be posed. Thus, we consider plane blades and acoustic sources concentrated at one point of the chord; only the span distributrion is introduced.

The expressions used in these conditions to describe the sound pressure on the harmonic of order $m$ at the frequency $f_m = mBN$ are written for the thickness term and the loading term, respectively, as

$$p_t = -\frac{\rho m^2 B^3 M_{\text{rot}}^2 R c^2}{4\pi S \beta^4}\left[1+\frac{MX}{S}\right]^2 \times \exp\left[-(imB\Omega/c\beta^2)(MX+S)\right]\exp\left[-imB(\varphi-\pi/2)\right] \times \int_0^1 \exp\left[imB\psi_0(z)\right]\cdot J_{mB}(mBM_{\text{rot}}Az) \times \left(\frac{b}{R}\right)^2 \int_0^1 xH(x)\,dx\,dz \quad (1)$$

$$p_l = \frac{imBM_{\text{rot}}}{4\pi Sc}\frac{W}{R}\exp\left[-(imB\Omega/c\beta^2)(MX+S)\right] \times \exp\left[-imB(\varphi-\pi/2)\right] \times \int_0^1\int_0^1 \left[\frac{1}{\beta^2}\left(M+\frac{X}{S}\right)\frac{\eta}{M}-\frac{1}{M_{\text{rot}}^2 z^2}\right] \times F(z)f(z,x)J_{mB}(mBM_{\text{rot}}Az)\exp\left[imB\psi_0(z)\right]dx\,dz \quad (2)$$

with $A=\sqrt{Y^2+Z^2}/S$ and $tg\varphi = Z/Y$.

Blade dimensions are expressed in reduced coordinates ($x=l/b$ for chord, $z=r/R$ for span), and observer location is defined by $X$, $A$, and $\varphi$. Other notations are given in the Nomenclature.

The computer code has been applied to three propellers defined by ONERA for the preliminary aircraft plans of Aerospatiale under certification-type conditions. Figure 1 shows an example of the results obtained for an overflight. We see, in particular, the beneficial effect of a high number of blades (propeller called HR2 less noisy than HR1) and of a lower rotation Mach number (HR2 quieter than HR3).

## III. Calculations of Far-Field Noise at Cruise Speed

In the case of cruising flight, the advancing Mach number is of the order of 0.7-0.8: the helical tip velocity becomes transonic, which generates very high noise levels a priori, such as to greatly interfere with the work of the crew. They even may cause this type of propulsion to be abandoned for passenger transport because a usual fuselage lining, which does not add too much to the weight of the aircraft, could be insufficient. An accurate noise prediction is therefore required. This is the reason why the preceding calculations, drawn up for conventional propellers, must be adapted to take into account the complicated shape of the blades and the noncompactness of the acoustic sources along the chord. It should be mentioned that these modifications have been made only on the thickness term, which, at the speeds under study, becomes predominant with respect to loading noise for single-rotating propellers.

### Noncompactness of Sources Along the Chord

We start again by considering plane blades and then introduce the phase shift that exists at a given span location between two points of the chord: $\epsilon(l,r) \simeq tg\epsilon = l/r$.

The expression of the thickness noise is then written as

$$p_t = -\frac{i\rho mB^2 M_{\text{rot}} R c^2}{4\pi S\beta^2}\left[1+\frac{MX}{S}\right] \times \exp\left[-(imB\Omega/c\beta^2)(MX+S)\right]\times\exp\left\{-imB[\psi-\pi/2]\right\} \times \int_0^1 \exp\left[imB\psi_0(z)\right]\sqrt{M^2+M_{\text{rot}}^2 z^2 J_{mB}}(mBM_{\text{rot}}Az)(b/R) \times \int_0^1 H'(x)\exp\left[imB(x/z)(b/R)\right]dx\,dz \quad (3)$$

In the case of transonic propellers, the emitted frequencies are such that the wavelengths are comparable to or less than the chord dimension. The phase term $\exp[imB(x/z)(b/R)]$ is other than unity; the acoustic sources radiating at the same

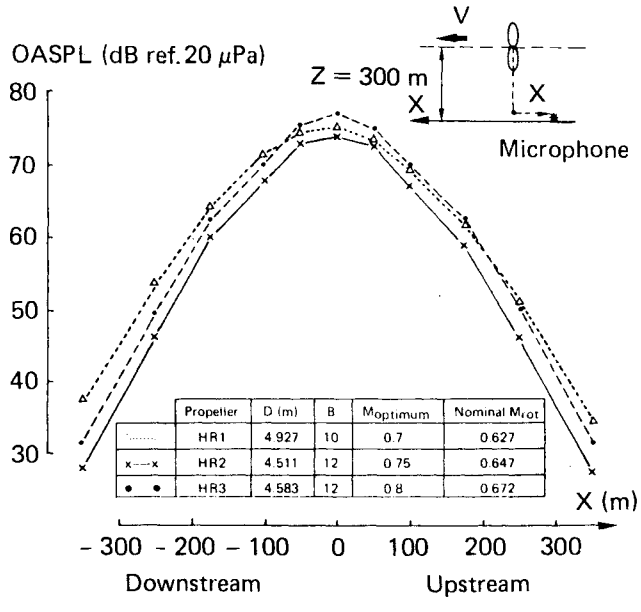


**Fig. 1 Overall sound level variation as a function of observation distance: $M=0.3$, nominal rotation speed, maximum power $W=W_{\max}=11{,}616$ kW (15,577 HP).**

time are perceived with a phase shift that tends to partially cancel their contribution. This is expressed (Fig. 2) by a sharper decrease of the sound spectrum with an already lower level at the blade passing frequency.

**Introduction of Blade Twist**

The following development permits us to avoid approximations that reduce the blades to one plane. Each point of a blade is located in a three-dimensional space (Fig. 3) and constitutes a sound source whose coordinates are written as

$$\left.\begin{matrix}\eta_1\\ \eta_2'\end{matrix}\right\}=\frac{1}{R}\left[\mp\left(1-\frac{b}{4}\right)\left\{\begin{matrix}\sin\\ \cos\end{matrix}\right\}(\beta+\phi)\mp y_L\left\{\begin{matrix}\sin\\ \cos\end{matrix}\right\}\phi\right] \quad \text{and} \quad \eta_3'=\frac{z_L}{R} \tag{4}$$

This code therefore generalizes the hypothesis of noncompactness along the chord. The expression for thickness noise takes the following form:

$$p_t=-i^{mB+1}\frac{\rho mB^2M_{\text{rot}}Rc^2}{4\pi S\beta^2}\times\int_0^1\int_0^1\sqrt{M^2+M_{\text{rot}}^2r^2}J_{mB}(mBM_{\text{rot}}A)\left(\frac{b}{R}\right)\times\frac{H'(x)}{\sqrt{1+H'(x)^2}}\circ\left[1+\frac{M(X-\eta_1R)}{S}\right]\times\exp(imBM_{\text{rot}}A_1)\times\exp(-imB\varphi)\,dx\,dr \tag{5}$$

with

$$r^2=\eta_2^2+\eta_3^2$$

$$A_1=\eta\left(M+\frac{X}{S}\right)\Big/\beta^2$$

$$A_2=(\eta_3Y-\eta_2Z)/S$$

$$A_3=(\eta_2Y+\eta_3Z)/S$$

$$A=\sqrt{A_2^2+A_3^2}$$

$$tg\varphi=A_3/A_2$$

The application of these expressions to the case of a 12-bladed propfan shows that the spectra are entirely comparable to those obtained by Eq. (3) if the helical tip Mach number is subsonic. In the transonic and supersonic domains (Figs. 2 and 4, respectively), differences appear on the spectra. Twist acts like noncompactness of the sources along the chord by introducing a phase shift between the various points of sound emission. The produced effect depends upon the ratio of the acoustic wavelengths ($\lambda=c/f$) and the characteristic dimensions of a blade; it can go as far as cancellation of certain waves. The result is therefore a reduction of sound levels. Taking blade twist into account for the calculation of thickness noise in transonic conditions is even more important for observation points located outside the plane of rotation of the propeller (Fig. 5). Thus, for a relative Mach number of 0.955 (Fig. 2), the difference on the blade passing frequency between the plane blade and twisted blade computations changes from 1 dB in the plane of rotation to 4 dB for an observation angle of 60 deg; differences can be much greater on the second harmonic.

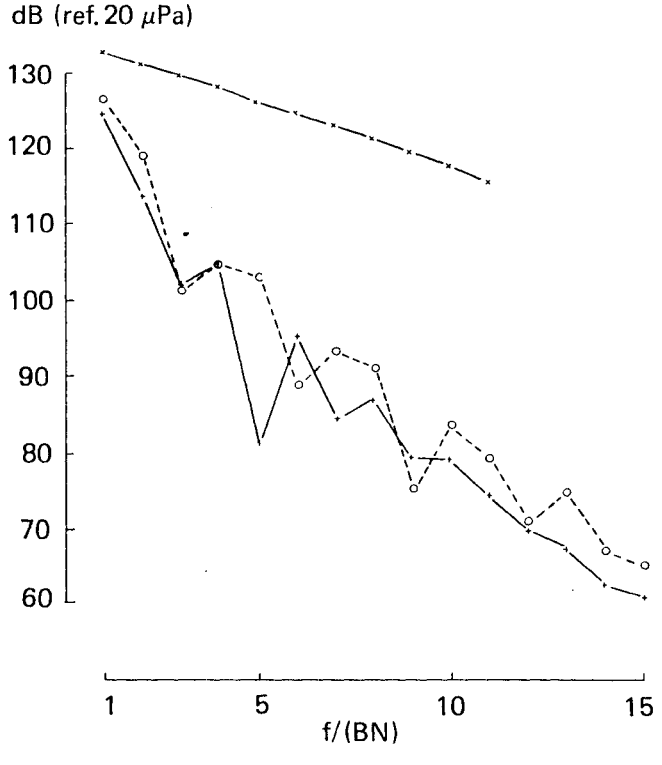


**Fig. 2 Comparison of the various hypotheses of thickness noise computation at transonic speed: $M_{\text{rel}}=0.95$ ($M=0.65$, $M_{\text{rot}}=0.7$). Sound spectra (tone noise) in the plane of the 12-bladed propeller at 3.D from the center: x–x plane blades, compact sources in chord; o--o plane blades, noncompact sources; +—+ twisted blades.**

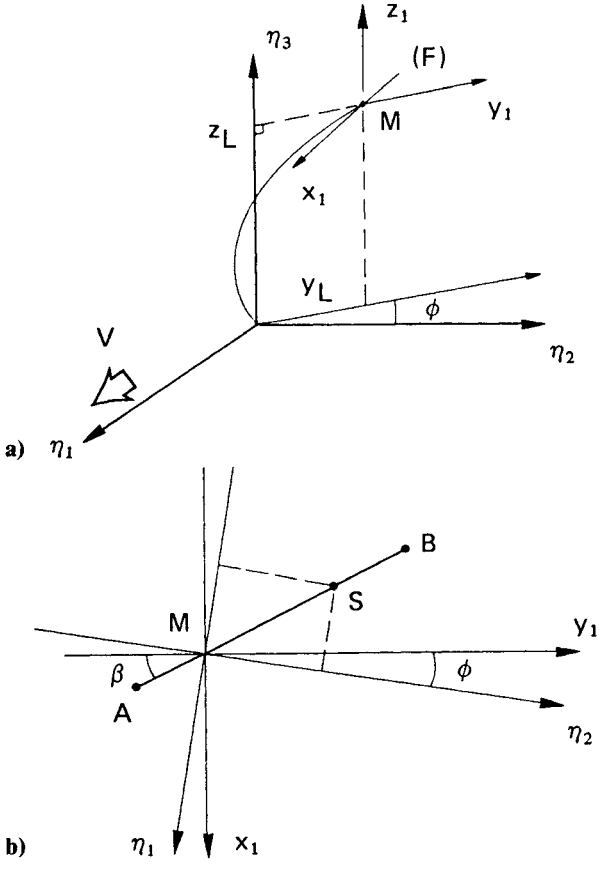


**Fig. 3 Identification of source points $S$ in three-dimensional space. a) Identification of the quarter-chord line $F$ ($M\epsilon F$), b) view in the plane $\eta_3=z_L$. $AB$ is the length of the chord at position $\eta_3=z_L$.**

Figure 6 shows some comparisons between computation of thickness noise with twisted blades [Eq. (5)] and theoretical and wind-tunnel results published by NASA.[16] Both U.S. and ONERA calculations (the first one in the time domain, the second one in the frequency domain) give similar variations of the sound level at the blade passing frequency as a function of the helical tip Mach number. For values lower than 1.1, experimental levels lie within the two types of computations. Similar results are found on higher harmonics (spectra computed at several Mach numbers). It should be noted that the observed differences could come, on the one hand, from a slight influence of loading noise, which is taken into account only in the NASA computation, and, on the other hand, from inaccuracies in the geometry of the blades entered as input of the ONERA code (U.S. propeller SR1 with eight blades).

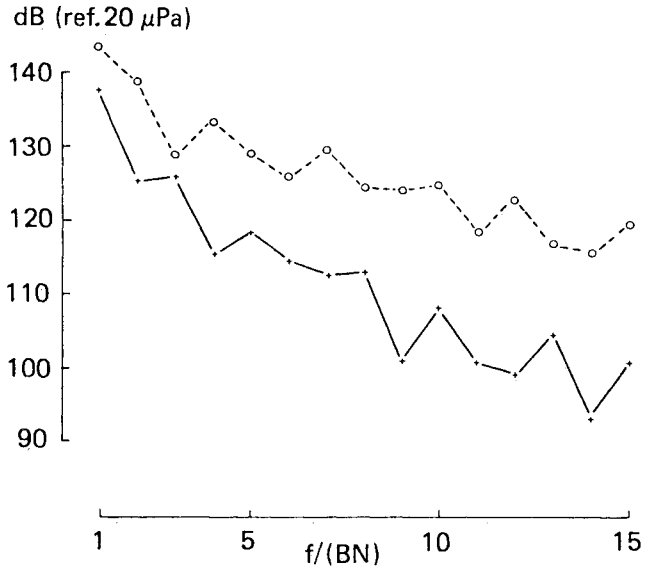


**Fig. 4 Comparison of thickness noise computations with noncompact sources at supersonic speed: $M_{rel}=1.06$ ($M=M_{rot}=0.75$). Sound spectra (tone noise) in the plane of the 12-bladed propeller at 3.D from the center: o---o plane blades; +—+ twisted blades.**

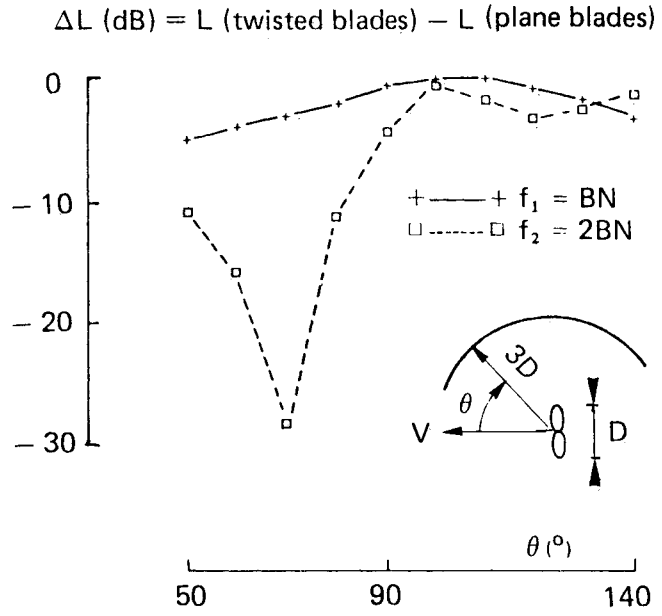


**Fig. 5 Effect of blade twist on the directivity of propeller noise (calculations with noncompact sources in both cases): $B=12$, $M_{rel}=0.955$ ($M=0.65$, $M_{rot}=0.7$).**

For the latter reason, such comparisons seem sufficient to validate the results previously discussed. However, it must be emphasized that some improvements of the NASA prediction methods were recently published,[17,18] but numerical results were given for propeller SR3 only. ONERA also continues its work in order to introduce the actual three-dimensional blade shape in the loading noise code, as was done for thickness noise. From an experimental point of view, in-flight tests were published,[19] but here again only propellers SR2 and SR3 were studied.

## IV. Near-Field Computations for Cruising Flight

In order to obtain information concerning noise levels at the fuselage location, which is at the limit of the far field of the propeller and sometimes even below, ONERA is presently investigating predictions with aerodynamic computations based on the Euler 3D equations[7]: pressure fluctuations are determined on and in the vicinity of the blades. They include all aerodynamic noise sources and, thus, permit access to the total sound level in the near field of the propeller; not only are the monopole and dipole terms taken into account, but also noise of quadrupolar origin disregarded in the computations presented in the preceding paragraphs.

### Sound Field Computation

The field of pressure fluctuations $p_j$ is obtained in a reference frame linked to the rotating blades by solving the Euler equations by a pseudo-unsteady method. For this purpose, a three-dimensional mesh is used on and near the blade.

For the acoustic computations, we consider only the points located beyond the radius of the blades. The angular distribution of pressure $p_j$ ($j$ from $j_{min}$ to $j_{max}$) being known over an arc of circle of $2\pi/B$ at a given axial position $X$ and distance $d$ to the axis, its average value $\bar{p}=(1/N)\Sigma_j p_j$ with $N=j_{max}-j_{min}$), and the discrete Fourier transform of the function $p(j)=p_j-\bar{p}$ are computed. The obtained spectrum $p_m(m=1,\ldots,(N-1)/2)$ describes the acoustic pressure of the harmonics of the propeller noise: at $f_m=mBN$, $L_m=10\log_{10}(|p_m|^2/p_{ref}^2)$ with $p_{ref}=20$ μPa, and the overall sound level is given by

$$L(\text{dB})=10\log_{10}\frac{p_{rms}^2}{p_{ref}^2}$$

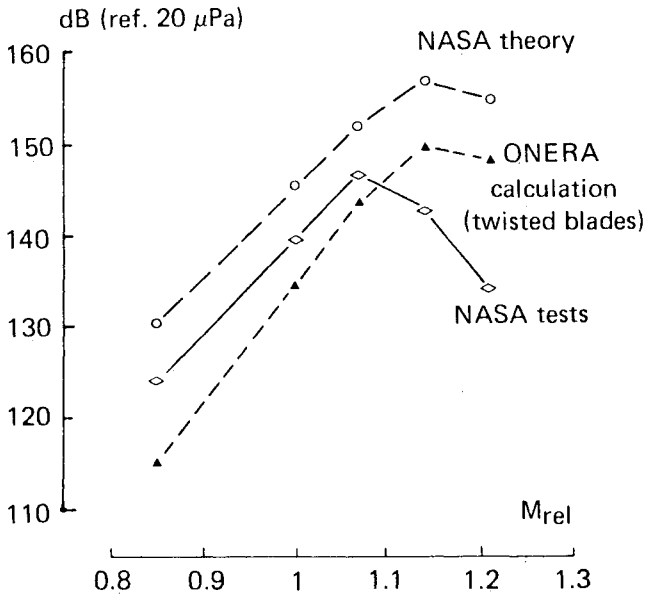


**Fig. 6 Noise level at the blade passing frequency $f_1=BN$ in the plane of rotation for the U.S. propeller SR1 ($B=8$).**

**Results Obtained**

The variation of the sound field, for observation points on a line parallel to the axis of rotation of the propeller, gives information on a fuselage that would be at a distance $d$ from the propeller axis. It is observed that the sound level is not maximum in the plane of the propeller ($X=0$), but slightly downstream. In the example of Fig. 7 ($d=1.45R$), the maximum sound emission angle is of the order of 100 deg. The sound level decreases very rapidly on both sides of this location because the effects of distance and directivity are combined. Computed spectra show a very strong dominance of the blade passing frequency; whatever the case examined (speed, point of observation), the difference between the first and the second acoustic harmonic is greater than 10 dB.

The idea to use the aerodynamic results of a Euler computation to evaluate sound levels is also used to advantage by Korkan and Von Lavante.[8] Figure 8 shows a comparison of the acoustic results as a function of distance $d$ in the plane of an eight-bladed propeller. Published data were obtained for SR3 and present data refer to a fictitious eight-bladed propeller. The lack of common parameters concerning blade geometry as well as power and advance ratio explains the bars on our results and makes the comparisons more qualitative than quantitative. We note, however, that the sound levels are of the same order of magnitude and that the decrease of the field with distance is similar; the sound pressure varies as about $1/d^5$ (attenuation of 30 dB when the distance is doubled) instead of $1/d$ in the far field.

It is necessary, however, to assess the validity of such an application of Euler codes for acoustic purposes. The finite size of the computation domain, with imposed pressure on the boundary, and the numerical viscosity, which must be introduced in order to obtain converging solutions, may partly explain the sharp decreases, both with frequency and distance. As a matter of fact, experiments of Brooks and Metzger[20] show shock waves (i.e., high frequencies) with a slow decrease around the propeller. This study is thus only beginning; in a second step, it is planned to extend the computation to observation distances farther away in order to examine the changes in the rate of decrease and to look for an overlapping with the far-field computations. In fact, tests of the SR6 propeller in the Boeing anechoic test chamber[21] and transonic wind tunnel[22] showed that the far-field hypotheses are valid whenever the distance $d$ reaches about 1.5–2 propeller diameters.

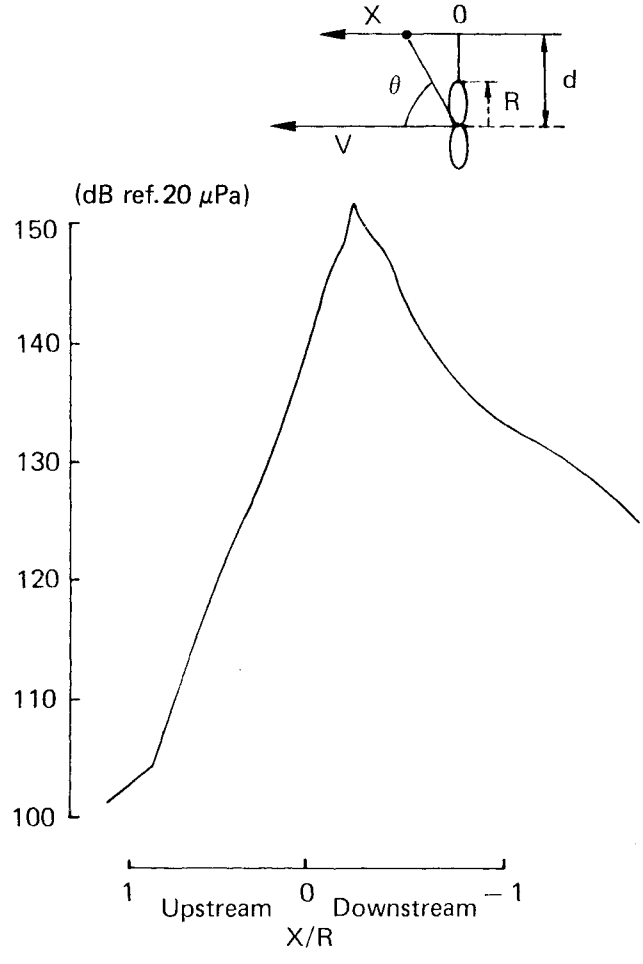


**Fig. 7 Variation of sound level at the blade passing frequency $f_1=BN$ obtained in the near field: $B=12$, $d/R=1.45$, $M_{rel}=1.06$.**

## V. Test at S1-MA

In October and November 1985, the testing of a 1-m-diam 12-bladed propfan model was carried out in the ONERA S1-MA wind tunnel in Modane-Avrieux (return-flow transonic wind tunnel with a closed test section of 8 m in diameter). The propfan, called HT3 (Fig. 9), is the scaled model of HR2 (see Fig. 1) defined by the ONERA

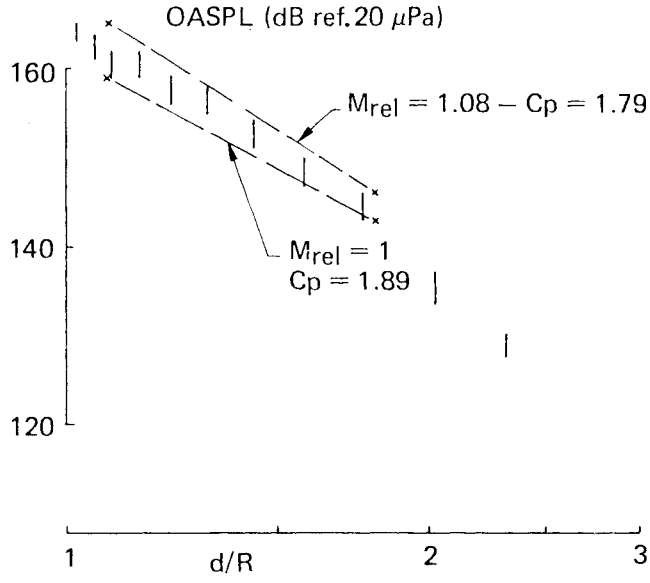


**Fig. 8 Computation of the near-field sound level in the plane of an eight-bladed propeller. Logarithmic scale in abscissa. x: Korkan and Van Lavante[8] results (propeller SR3); Advance ratio $J=3.06$. |: ONERA results; $M_{rel}=1.06$, $J=3.15$, power coefficient $1.81<C_p<2.18$.**

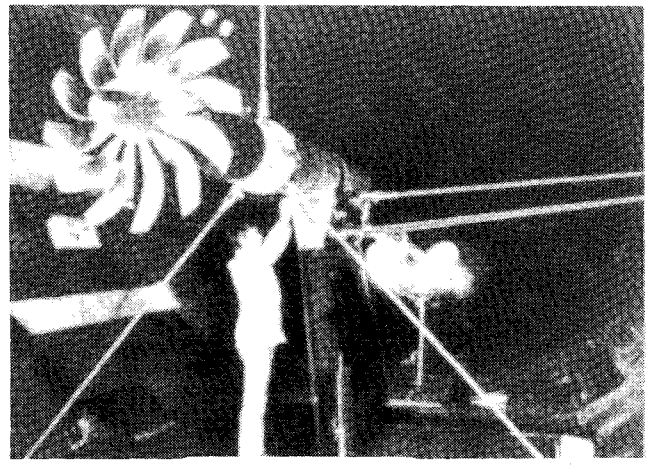

**Fig. 9 Assembly view of propfan model setup in the test section of the S1-MA wind tunnel.**

Aerodynamics Department for an optimum cruise Mach number of 0.75. It was manufactured and equipped with Kulite pressure transducers by the Helicopter Division of Aerospatiale and was driven by a motor designed and produced by the Large Testing Facilities Department of ONERA and by Ratier-Figeac.

Along with the measurements of the propfan performance and blade aeroelasticity, which constituted the main objective of this program, acoustic measurements were taken, in spite of the absence of acoustic lining on the walls of the test section.

#### Description of Acoustic Measurements

The axis of the propfan was located 1.20 m below that of the test section. This off-center position of the propfan is advantageous for acoustic measurements because it prevents the refocusing of the sound waves on the source, which might occur without acoustic lining.

The main problem encountered in the preparation of these tests was to make suitable acoustic measurements at high velocity, up to a Mach number of 0.75. Three microphones were placed at the wall of the test section, but the acoustic waves risk being disturbed crossing the boundary layer.[23] In order also to put the transducers closer to the model, we used waveguide probes (Fig. 10), inspired by those developed for lower speeds by the Acoustics Department of SNECMA, for its studies of propagation in turbojet exhaust ducts. A probe of this type was placed near a flush-mounted transducers but with the pressure tube outside the boundary layer, in order to assess the effect of the boundary layer and of reflections on the walls. Six other probes mounted in streamlined masts were positioned in the flow at various distances from the propfan and at several angular locations. The microphone closest to the propfan is at $d = 1.6$ m from the center (thus 1.6 diameters). So it is agreed that the 10 microphones are in the far field with respect to the acoustic source.[21,22]

The tests were carried out for flow Mach numbers between 0.25 and 0.75, without any propeller incidence.

#### Behavior of the Results

The signals recorded in a bandwidth of 0–20 kHz are analyzed with a frequency resolution of 25 Hz; the spectra are plotted in the 0–10-kHz band.

Overall, whatever the flow speed and microphone considered, the propeller pure tones emerge from the broadband noise. For the lowest flow speeds ($M \leq 0.6$), besides the propeller pure tones, tones appear on the spectra (Fig. 11) due to the presence of shrouds visible on Fig. 9; their frequencies are actually proportional to the flow speed. At $M = 0.5$, the analysis of the spectra is rendered difficult by the presence of these tones: the blade passing frequency, at $f_1 = BN$, is very close to the tone due to the shroud of 35 mm in diameter and its sound level is lower. At the highest speeds ($M > 0.6$), the tones due to the presence of the shrouds are buried in the broadband noise (Fig. 12) and, in spite of the very strong increase of the latter (~20 dB between $M = 0.25$ and 0.75), the propeller pure tones, or at least the first one, emerge clearly.

In addition, we observe that, at least on the blade passing frequency at $f_1 = BN \simeq 1$ kHz, the signals picked by the flush-mounted transducers do not seem to be affected by the boundary layer and that of the probe near the wall do not appear to be disturbed by reflection phenomena: the difference in sound level on this tone, $f_1 = \mathrm{BN}$, is on the order of 6 dB, which corresponds to the doubling expected from the sound pressure on a wall. The effect of the wall boundary layer may be greater for the higher harmonics because their wavelengths become smaller than the thickness of the boundary layer. The conclusions concerning reflection, drawn from microphones located in the plane of the propeller, should also be moderated for measurements rather distant upstream or downstream, as mentioned in the following paragraph. In addition, a confinement effect is visible in some cases because microphones farther away from the propeller can perceive more noise than others closer to it.

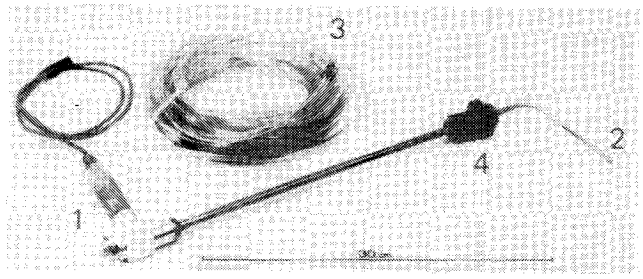


**Fig. 10 View of microphone probe for high-speed flow: 1—Brüel and Kjaer, microphone and adapter; 2—static pressure tube; 3—Antireflection coiled tube; 4—wall-mounting clip (used only for the probe without mast).**

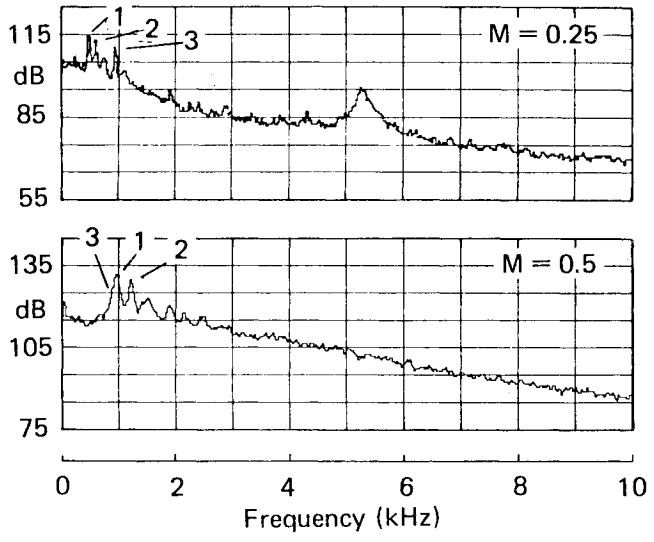


**Fig. 11 Spectra obtained at low speed. Microphone in the propeller plane at $d = 3.5$ m: 1—shroud $\phi = 35$ mm, 2—shroud $\phi = 30$ mm, 3—blade passing frequency $f_1 = BN$.**

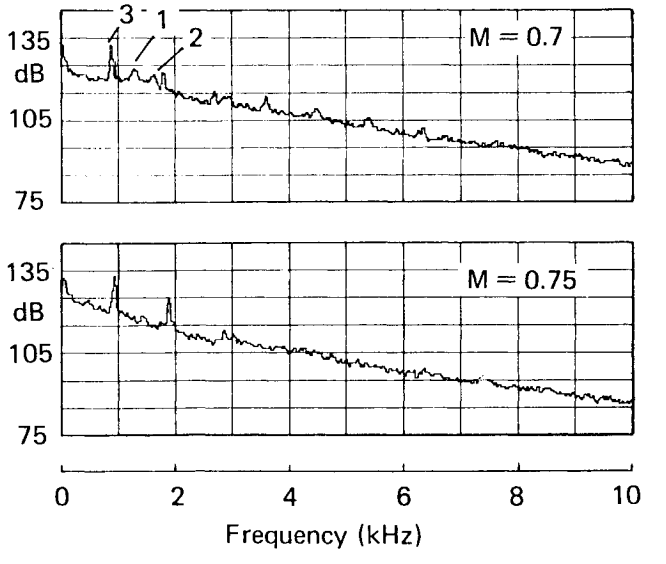


**Fig. 12 Spectrum obtained at high speed. Microphone in the propeller plane at $d = 3.5$ m: 1—shroud $\phi = 35$ mm, 2—shroud $\phi = 30$ mm, 3—blade passing frequency $f_1 = BN$.**

**Preliminary Comparisons with Theoretical Results**

For these first comparisons, we use the computational model of the far-field type, with the hypotheses of plane blades and noncompact sources, which takes into account the thickness and mean loading noise (relations 2 and 3). The following comparisons concern only sound levels at the blade passing frequency, $f_1 = BN$ (Fig. 13).

1) For microphones located in the plane of the propeller ($\theta = 90$ deg), the computation and the corresponding test are in good agreement except at maximum speed ($M_{rel} = 1.04$), where the theory greatly overestimates the sound levels; the model taking into account the twisted shape of the blades would lead to a decrease of sound levels and, therefore, improve the agreement with the experimental results at relative transonic speeds.

2) For the microphones placed rather far away upstream and downstream from the plane of the propeller, very large differences appear between the theoretical and experimental results; the computed sound levels are always lower. An explanation, at least partial, may lie in the absence of acoustic lining: since sound emission is maximum around the plane of the propeller, the wall reflections can produce an appreciable increase in the noise perceived upstream and downstream.

## VI. Conclusion

The acoustic study of propfans has been undertaken at ONERA within the framework of research on this type of propellers, carried out in France for several years. The application of noise prediction codes, developed for conventional propellers, has served to estimate sound levels radiated by three propfans under conditions of certification (low speeds, far field). These data are used by Aerospatiale for aircraft preliminary plans.

In the case of cruising flight in which relative blade-tip velocities become transonic, the far-field noise computations have been improved to take into account the exact shape of the blades and the distribution of acoustic sources along the chord. These modifications are appreciable when the acoustic wavelengths become comparable to the blade dimensions; the phase shifts created are then important and some waves can be practically canceled. This results in lower sound levels and a spectrum decrease sharper than in the case of the simplified computation. The work carried out on thickness noise will be extended to the computation of loading noise: if the latter is low for single-rotating propellers in cruising flight, it increases for counterrotating propellers and unducted fans because of fluctuations due to the interactions.

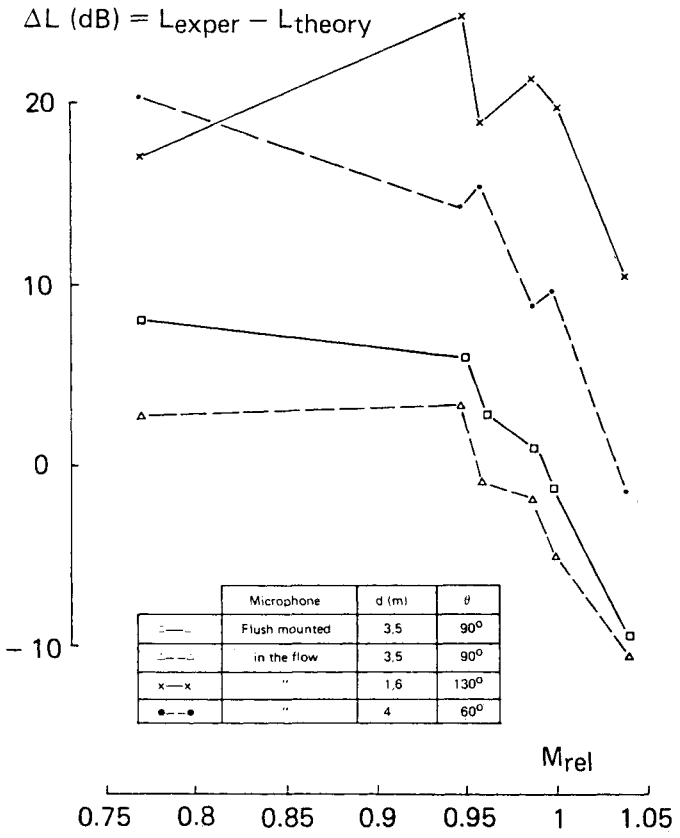


**Fig. 13 Comparison of experimental and theoretical results at the blade passing frequency $f_1 = BN$.**

In order to be able to obtain near-field information including all of the sources of aerodynamic noise, acoustic computations are carried out based on the pressure fluctuations given by the solution of the Euler 3D equations. In the vicinity of the blades, the sound level is maximum for an observer location slightly downstream of the plane of rotation of the propeller. The rate of decrease of sound pressure with distance is much higher than in the far field since an attenuation of 30 dB is observed when the observation distance is doubled, instead of 6 dB. This first study will be followed up mainly by extending the computation domain in order to be able to make the connection between the near and far fields.

Tests of a transonic propfan model in the S1-MA wind tunnel have permitted a data base on this type of propeller to be constituted. In spite of the differences with theoretical results, due especially to the absence of acoustic lining on the walls of the wind tunnel, the first comparisons are encouraging and new tests with propeller incidence and at higher flow speeds ($M = 0.8$) are also planned.

## Acknowledgments

This study was carried out under contract with the Direction des Recherches, Etudes et Techniques and the Service Technique des Programmes Aéronautiques. The authors would like to express their thanks to the Aerodynamics Department of ONERA for the support offered for this work, and especially to J. M. Bousquet, who directs the engineering studies of ONERA on propfans and who executed the Euler computations used for the near-field noise prediction.

## References

[1]Bousquet, J.M., "Hélices pour vol économique a grandes vitesses," *l'Aéronautique et l'Astronautique,* No. 88, 1981-3, pp. 37-51.

[2]Arndt, W.E., "Propfans Go Full Scale," *Aerospace America,* Jan. 1984, pp. 100-103.

[3]Dahan, C., "Propeller Light Aircraft Noise at Discrete Frequencies," *Journal of Aircraft,* Vol. 18, June 1980, pp. 480-486.

[4]Gounet, H., "Contribution to the Study of Light Aircraft Propeller Noise," ONERA, NT 1982-8.

[5]Hanson, D.B. and Fink, M.R., "The Importance of Quadrupole Sources in Prediction of Transonic Tip Speed Propeller Noise," *Journal of Sound and Vibration,* Vol. 62, Jan. 1979, pp. 19-38.

[6]Prieur, J., "Calculations of Transonic Rotor Noise Using a Frequency Domain Formulation," AIAA Paper 86-1901, July 1986.

[7]Bousquet, J.M., "Aerodynamic Methods Used in France for Designing Advanced High-Speed Propellers," *Aerodynamics and Acoustics of Propellers,* AGARD CP-366, Oct. 1984, Ref. 2.

[8]Korkan, K.D. and Von Lavante, E., "An Alternative Method of Calculating Propeller Noise Generated at Transonic Tip Speeds, Including Non-Linear Effects," AIAA Paper 85-0002, Jan. 1985.

[9]Goldstein, M.E., *Aeroacoustics,* McGraw-Hill, New York, 1976.

[10]Hanson, D.B., "Influence of Propeller Design Parameters on Far-Field Harmonic Noise in Forward Flight," *AIAA Journal,* Vol. 18, Nov. 1980, pp. 1313-1319.

[11]Legendre, R., "Noise Generated by a Propeller or a Helicopter Rotor," *La Recherche Aérospatiale,* No. 1982-3 (English edition), May-June 1982, pp. 1-5.

[12]Tam, C.K.W. and Salikuddin, M., "Weakly Nonlinear Acoustic and Shock-Wave Theory of the Noise of Advanced High-Speed Tur-

bopropellers," *Journal of Fluid Mechanics,* Vol. 164, March 1986, pp. 127-154.

[13]Farassat, F. and Succi, G.P., "A Review of Propeller Discrete Frequency Noise Prediction Technology with Emphasis on Two Current Methods for Time Domain Calculations," *Journal of Sound and Vibration,* Vol. 71, No. 3, Aug. 1980, pp. 399-419.

[14]Padula, S.L. and Block, P.J.W., "Acoustic Prediction Methods for the NASA Generalized Advanced Propeller Analysis System (GAPAS)," AIAA Paper 84-2243, July 1984.

[15]Azuma, A., Kawachi, P., Watanabe, T., and Nakamura, Y., "Performance and Noise Analysis of Advanced Turboprop," 11th European Rotorcraft Forum, Paper 11, Sept. 1985.

[16]Dittmar, J.H., "A Comparison Between an Existing Propeller Noise Theory and Wind Tunnel Data," NASA TM-81519, 1980.

[17]Farassat, F., "The Unified Acoustic and Aerodynamic Prediction Theory of Advanced Propellers in the Time Domain," *AIAA Journal,* Vol. 24, April 1986, pp. 578-584.

[18]Farassat, F., Dunn, M.H., and Padula, S.L., "Advanced Turboprop Noise Prediction—Development of a Code at NASA Langley Based on Recent Theoretical Results," NASA TM-88993, July 1986.

[19]Brooks, B.M. and Mackhall, K.G., "Measurement and Analysis of Acoustic Test Data for Two Advanced Design High Speed Propeller Models," AIAA Paper 84-0250, Jan. 1984.

[20]Brooks, B.M. and Metzger, F.B., "Acoustic Test and Analysis of Three Advanced Turboprop Models," NASA CR-159667, Jan. 1980.

[21]Plunkett, E.I., Topness, P.C., and Simcox, C.D., "Noise Testing of an Advanced Design Propeller in the Boeing Anechoic Test Chamber with a Relative Velocity Free Jet," AIAA Paper 84-2262, Oct. 1984.

[22]Glover, B.M. Jr., Plunkett, E.I., and Simcox, C.D., "Noise Testing of an Advanced Design Propeller in the Boeing Transonic Wind Tunnel With and Without Test Section Acoustic Treatment," AIAA Paper 84-2366, Oct. 1984.

[23]Dittmar, J.H., "Experimental Investigation of the Effect of Boundary Layer Refraction on the Noise from High Speed Propeller," NASA TM-83764, Sept. 1984.